JCTC Journal of Chemical Theory and Computation

Article

pubs.acs.org/JCTC

A Composite Energy Treatment for Sterically Hindered Cluster Models for the Si(100) Surface

Benjamin C. Gamoke, Nicholas J. Mayhall, and Krishnan Raghavachari*

Department of Chemistry, Indiana University, Bloomington, Indiana 47405, United States

Supporting Information

ABSTRACT: Cluster models representing multiple dimer rows on the Si(100) surface suffer from unfavorable and unphysical steric interactions between hydrogen link atoms. A novel composite energy method is proposed to cancel such undesirable interactions present in the cluster model. In our composite method, the unphysical repulsive interaction energy between excised fragments (defined from the cluster model) is replaced by individual noninteracting fragments along with a Lennard-Jones-type repulsion term between the neighboring link atoms. The resulting composite energy and the associated gradients consist of well-defined individual subsystem calculations and can be used to perform geometry optimizations using such cluster models without additional constraints. Despite small differences from an ideal Si(100) reconstructed surface, this model can be used to investigate and analyze important surface chemical reactions. Results of allylic mercaptan adsorption on a Si(100) dimer using our proposed cluster model are reported to demonstrate the novel method's robustness.

1. INTRODUCTION

Silicon has been the primary material for the semiconductor and electronics industries, and extensive research is being carried out on functionalized silicon surfaces for potential applications in many areas of technology. The two most important systems for silicon surface chemistry are the Si(100) and Si(111) surfaces. The Si(111) surface, when hydrogenated or etched under mild conditions, creates an atomically flat surface.[1] The Si(100) surface reconstructs to form dimer rows that are preserved upon hydrogen termination. Both of these surfaces can be modified for reactivity studies by creating a localized radical site, e.g., through the use of an STM tip.[2] Many adsorption studies have been performed experimentally and theoretically for understanding functionalized silicon surfaces.

Computational investigations of silicon surface chemistry are commonly carried out either using a slab approach (periodic boundary conditions) or the alternative cluster approach. For localized chemistry, cluster models that provide an accurate description of the local region of interaction and its immediate environment are an appropriate choice.[3] The basic cluster model is first defined from a bulk structure and the surface reactive site. The dangling bonds resulting from any broken bulk Si−Si bonds are then terminated with hydrogen "link" atoms to avoid any artifacts due to excess spin or charge. Additionally, constraints may be applied to make the cluster model have more appropriate boundary effects. Cluster models are advantageous for use in many surface reactivity studies because they can be treated exactly like a finite molecule, unlike slab calculations, where methods that calculate exact exchange, such has HF, MP2, or B3LYP, are prohibitively expensive for large unit cells. Computationally, cluster models are significantly more efficient for surface reactivity studies because sufficiently large unit cells must be employed to ignore intercell adsorbate interactions.

The focus in this work is on Si(100), the surface of importance in microelectronics. Cluster models require a finite truncation of the Si(100) surface and, when appropriately chosen, can lead to reactivity and behavior in agreement with experimental results. However, without careful treatment, the standard cluster methods for modeling the Si(100) surface can potentially lead to significant problems. This is particularly true for larger clusters that contain multiple surface dimers along and across dimer rows.

The potential problems for the Si(100) surface can be illustrated with the model shown in Figure 1. The surface

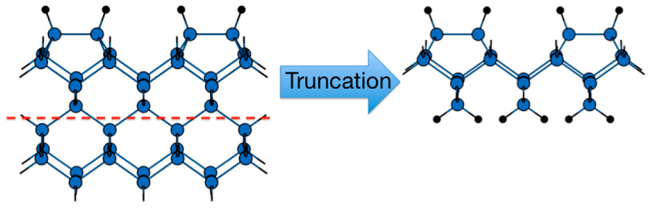

Figure 1. Model illustrating potential problems for the Si(100) surface. Starting from a model representing the reconstructed Si(100) surface (left), truncation of the surface at the fourth layer using a standard hydrogen link atom termination leads to the cluster model (right). Silicon atoms are in blue and hydrogen atoms are in black.

shown has two dimers in adjacent rows that can describe chemical reactions (*vide infra*) when interactions between neighboring dimers are significant. The ideal surface is shown on the left, and a truncated cluster model that is terminated at the fourth layer is shown on the right. The main reason for the problem is that truncation of the bonds between two layers of a Si(100) surface leads to *two covalent bonds being severed to the same atom* in the lower layer. If both broken bonds are

Special Issue: Berny Schlegel Festschrift

Received: August 17, 2012
Published: October 11, 2012

dx.doi.org/10.1021/ct3007259 | J. Chem. Theory Comput. 2012, 8, 5132−5136

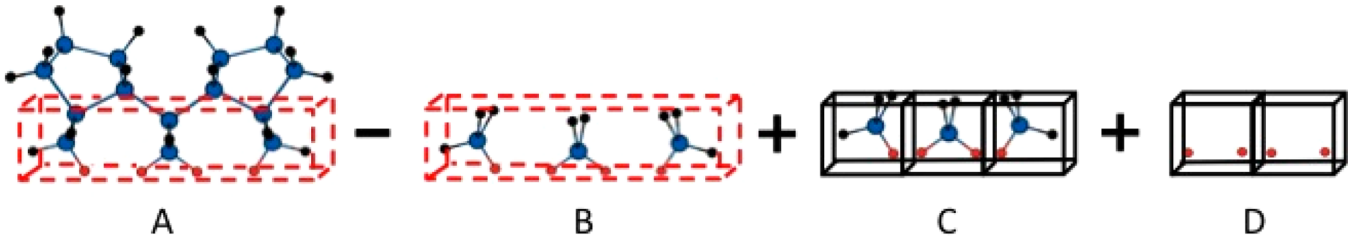

Figure 2. The hybrid energy scheme proposed for removing spurious repulsive intramolecular hydrogen interactions. The composite energy and gradient are evaluated as a sum of the energy and forces of each subsystem. Appropriate link atom scale factors must be used to terminate the broken bonds. Silicon atoms are in blue, and hydrogen atoms are in black and red. Red hydrogen atoms contribute to the unphysical repulsive interactions of the silicon cluster.

terminated with hydrogen atoms, the two capping hydrogen atoms (that both represent the same original silicon atom) will be ~1.4−1.5 Å apart, resulting in repulsive H···H interactions, as the two atoms are significantly closer than the sum of their van der Waals radii (2.4 Å). Such an interaction is clearly unphysical, arising only because of truncation. If such a terminated structure is optimized without constraints, substantial geometrical distortions occur, as the hydrogen atoms optimize to a H···H distance of 2.475 Å at the B3LYP/6-31G(d,p) level.

There are several potential solutions to this problem. The cluster can be extended to deeper layers leading to a tapered structure that avoids such interactions, at the expense of larger computational cost. A second solution is to truncate with divalent "pseudoatoms" instead of monovalent hydrogen atoms. A more common solution is to sidestep the problem by freezing the atoms of the lower layers in performing geometry optimizations to avoid the unphysical artifacts that could lead to distorted geometries.

In this paper, a new composite method is proposed that allows for the selective removal of the effects of the unphysical steric interaction. It uses concepts similar in spirit to the ONIOM[4−6] method that uses a hybrid potential energy surface. However, instead of combining multiple levels of theory in different regions as in standard ONIOM, we define a hybrid energy in our method that purposefully attempts to remove the relevant interactions by canceling them via a series of independent calculations at a fixed level of theory. The hybrid potential energy can be minimized with respect to geometrical parameters to find meaningful structures, minima that reflect how a system would behave without the presence of the forces that would otherwise exist in a standard calculation.

2. METHOD

To overcome this unphysical distortion due to truncation in the Si(100) surface, a hybrid energy scheme is defined as shown in Figure 2. In this composite energy, undesirable interactions present in the full system (A) are canceled by the interaction energy between excised fragments defined from the full system (B) and replaced by the individual noninteracting equivalent fragments (C). In a similar manner to the composite energy defined in our PBC-LC method,[7] as a starting point the composite energy can be defined in eq 1 as

$$E(\text{composite}) = E_{\text{full}} - E_{\text{model,interacting}} + \sum E_{\text{model,noninteracting}} \quad (1)$$

In this particular example, such a composite energy expression requires five separate subsystem calculations, all of which are dependent upon the geometry of the full cluster at each energy evaluation. In other words, each individual subsystem has a geometry (e.g., Cartesian coordinates) that is derived from the coordinates of the full molecular system at the current optimization step. Apart from the full molecular system calculation (E_{full}), the remaining four subsystem calculations are performed on the smaller models (derived from the full system) and add very little overhead to the overall computational expense. Note that link atom terminations are used for each of the subsystems that involve broken covalent bonds. The link atoms (hydrogens) replace the corresponding silicon atoms, but bond lengths are shortened by a constant scale factor (0.61) to reflect the fact that Si−H bonds are much shorter than Si−Si bonds.

However, there can be a potential problem when applying eq 1 to geometry optimizations. This is due to a possible imbalance between the repulsive interactions in the full system and the model system, as they may not cancel exactly since they represent similar, but not identical, structural entities. This may cause a deficiency in representing the energy and gradient of the molecular system at certain geometries where $E_{\text{model,interacting}}$ strongly dominates as a highly repulsive term (e.g., by portions of the model system coming in close proximity to each other). Since $E_{\text{model,interacting}}$ is included with a negative sign, E(composite) is lowered, and this may lead to a collapse of the hydrogens toward each other. To avoid this, we have included a fitted van der Waals-type repulsive term that prevents such nonbonded hydrogens from getting too close. Thus, we define a final modified composite energy expression defined in eq 2.

$$E(\text{composite}) = E_{\text{full}} - E_{\text{model,interacting}} - \sum E_{\text{model,noninteracting}} + \sum E_{\text{H···H Correction}} \quad (2)$$

In eq 2, an additional term, $\sum E_{\text{H···H Correction}}$, is added to the energy of the full molecular system. This correction (Figure 2d), which adds a (fitted) repulsive van der Waals interaction between nonbonded H···H pairs in the model system, is a key component for obtaining reasonable chemical structures. In the case of the Si(100) cluster at the B3LYP/6-31G(d,p) level, we implemented this by replacing the Lennard-Jones parameters of the Dreiding force field[8] with new parameters (R_0 = 4.0 Å, D_0 = 1×10^{-6} kcal/mol). The parameters were adjusted to yield a reasonably shaped potential curve (i.e., relaxed scan) as a function of the H···H distance with a single minimum at a value close to the expected value of 1.4−1.5 Å.

dx.doi.org/10.1021/ct3007259 | J. Chem. Theory Comput. 2012, 8, 5132−5136

Since the composite energy is the sum of the energies of independent subcalculations, the corresponding gradients required for geometry optimization can also be defined in a similar manner, requiring only independent subcalculations. Additionally, since the spurious interaction has been canceled in the composite energy, unconstrained optimization of the transition state and ground state geometries on this new composite potential energy surface are well-defined and can be performed with a standard geometry optimizer. In the case of the Si(100) surface, the optimized geometry for the cluster without any constraints yields the structure shown in the top portion of Figure 3. The structure is distorted strongly at the bottom layer due to the unfavorable steric repulsions and is clearly not representative of the real surface. Using the expression in eq 2, the cluster is described quite well (Figure 3, bottom). The geometry relaxes, allowing for H···H distances of 1.454 Å that are very close to the expected value. The corresponding potential energy curve is given as Figure S1 in the Supporting Information. At the optimized geometry, the bottom layer is quite flat while the curvature of the surface is considerably minimized. The Si−Si dimers located at the reconstruction of the Si(100) cluster are slightly tilted inward across dimer rows. Despite these small differences from an ideal Si(100) reconstructed surface, this model can be used to analyze important surface chemistry without the application of any constraints.

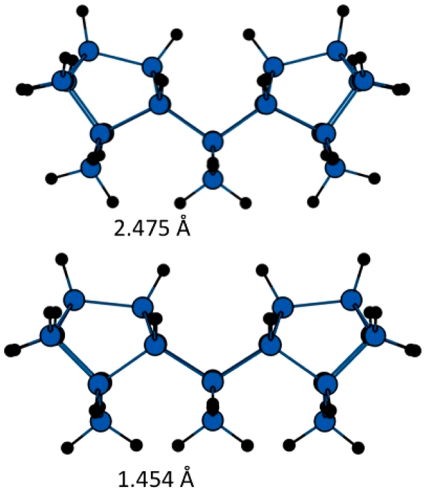

Figure 3. Optimized Si(100) cluster geometries at the B3LYP/6-31G(d,p) level of theory. Silicon atoms are in blue, and hydrogen atoms are in black. A standard geometry optimization (top) leads to geometrical distortions, with bottom layer H···H distances at 2.475 Å. Geometry optimization utilizing our proposed composite energy scheme (bottom) has a minimum with bottom layer H···H distances at 1.454 Å.

3. COMPUTATIONAL DETAILS

All calculations were performed using the Gaussian Development Version[9] program package. The level of theory used in all the optimization of Si(100) clusters was B3LYP[10−12]/6-31G(d,p).[13−15] A scale factor of 0.61 was used to determine the bond lengths involving link atoms (i.e., ratio of the bond lengths Si−H/Si−Si = 0.61).

4. ROBUSTNESS OF THE METHOD

Patterned line growth of allylic mercaptan (ALM) on the Si(100) surface has been of considerable interest in the silicon semiconductor surface community.[16−18] The line growth reactions result from radical-initiated chain reactions and have been investigated for many adsorbates. While many adsorbates undergo chain reactions *along* dimer rows, ALM reacts *across* dimer rows, leading to novel patterns on the Si(100) surface. We demonstrate the robustness of our method by efficiently using it to study surface reactions concerning such mechanisms.

In previous work, Ferguson et al.[19,20] used cluster models to theoretically investigate possible mechanisms for radical initiated line growth across silicon dimer rows. The cluster models that were used to study these geometries required freezing the coordinates of all of the silicon atoms except for the top two layers in the model; this is a dramatically large constraint. However, such freezing of atoms was employed to ensure that large and unphysical geometric distortions are avoided. Our interaction deletion method provides an efficient alternative to overcome such severe unphysical constraints.

The first step in the line growth process across the Si dimers is the adsorption of ALM on a Si(100) surface at a localized radical site. Two products are possible at this step: one with a primary carbon radical (labeled "branched") and another with a secondary carbon radical (labeled "linear"). We have optimized the two possible initial adsorption products from the interaction of ALM with a surface radical site (Figure 4). Reasonable geometries are obtained for both structures with our composite energy approach.

Further, our method is useful for studying transition states as well. In the complete reaction mechanism, the carbon radical (branched or linear) rearranges to a sulfur radical (not shown). This is followed by an important step involved in the line growth, *viz.* a hydrogen atom abstraction reaction involving an interdimer transition state. It involves the sulfur radical, in either a linear or branched structure, capturing a hydrogen atom from the neighboring dimer, breaking the Si−H bond, and creating a silicon radical localized on the adjacent dimer. The reactant, transition state, and product, obtained for both the branched and linear reaction pathways, are shown in (Figure 5). In all cases, our composite energy model has been employed to obtain the optimized geometries.

Since our composite energy method effectively removes the unphysical hydrogen−hydrogen interactions, reasonable adsorbate geometries are obtained in all cases, including the transition states. The large buckling obtained in the unconstrained model is avoided for all the structures. The stretched S···H and H···Si distances are described appropriately in our model with minimal distortion from the bottom layer of the four-layer Si(100) cluster model. This suggests that our Lennard-Jones-type parameters are transferable across the potential energy surface.

Energetically, our method is in agreement with the previous work of Ferguson et al.[19] A 5.7 kcal/mol difference is obtained between the branched and linear initial adsorbates (Figure 4), with the linear structure being preferred. This is very close to the value obtained previously with the constrained model (5.4 kcal/mol) as well as that with an unconstrained cluster (5.7 kcal/mol). The close agreement between the different models is consistent with the fact that the structures all occur within a single dimer and may not be sensitive to the presence of surface strain.

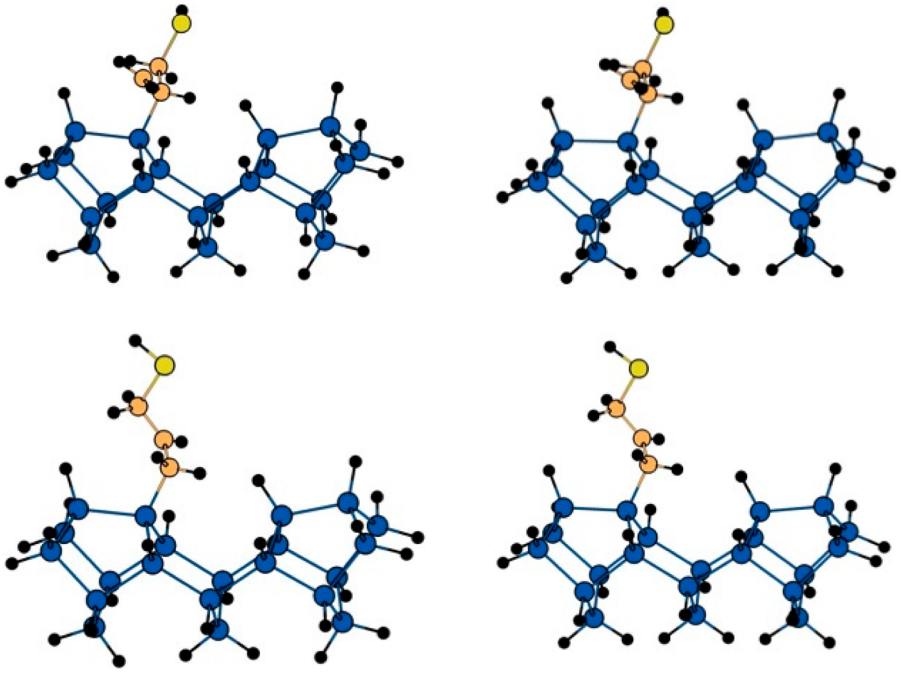

Figure 4. Optimized branched (top) and linear (bottom) allylic mercaptan adsorbate on Si(100) using a standard optimization procedure (left) and our defined hybrid energy method (right). Sulfur, carbon, silicon, and hydrogen are shown in yellow, orange, blue, and black, respectively.

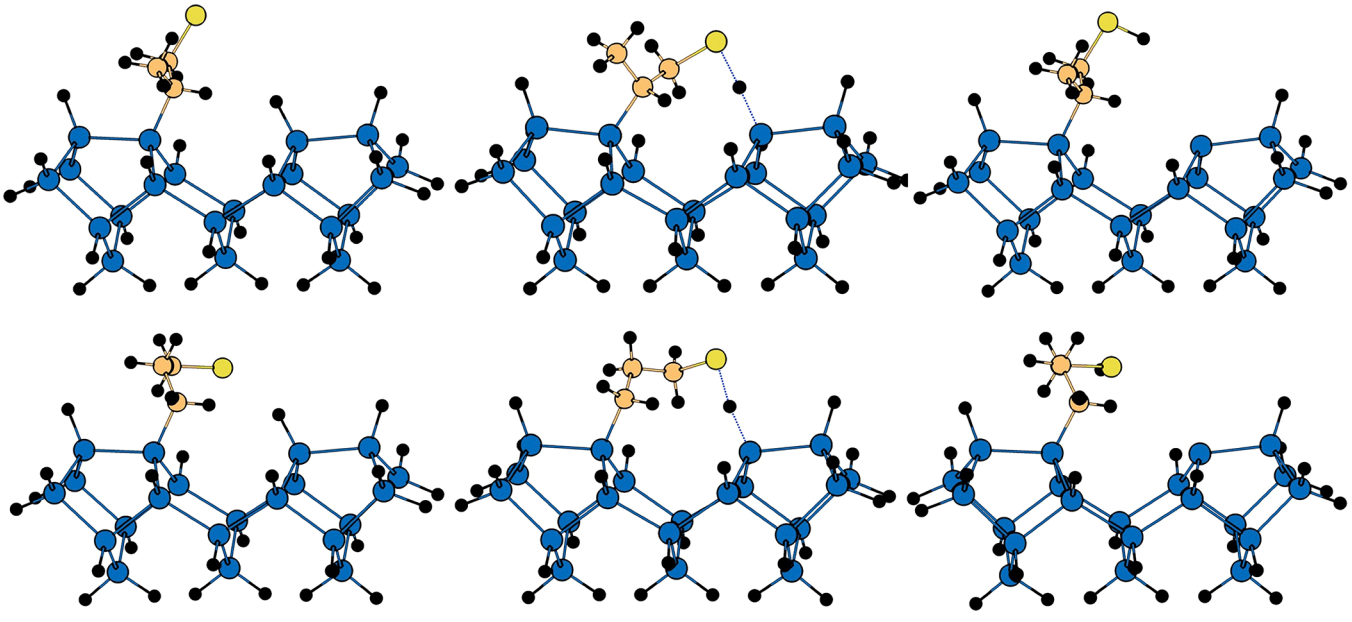

Figure 5. Optimized reactant (left), transition state (middle), and product (right), along hydrogen abstraction reaction coordinate with branched (top) and linear (bottom) allylic mercaptan on Si(100) using our defined hybrid energy method. Sulfur, carbon, silicon, and hydrogen are shown in yellow, orange, blue, and black, respectivly.

The transition state barrier height for the hydrogen abstraction process from an initial branched adsorbate (Figure 5) is 5.8 kcal/mol. This is within 1 kcal/mol of the value reported with the constrained cluster model (6.6 kcal/mol). Similarly, the linear adsorbate leads to a barrier height of 3.6 kcal/mol and is in reasonable agreement with the 2.2 kcal/mol calculated from the constrained cluster model. However, the relative energy barrier between the branched and linear adsorbate structures changes significantly from 2.2 kcal/mol (current model) to 4.4 kcal/mol (constrained model). Interestingly, the unconstrained cluster model calculations predict barrier heights (5.0 and 3.3 kcal/mol, respectively, for branched and linear adsorbates) that are quite close to our new model. While the current results suggest that the previous models perform satisfactorily for this system, larger differences between the different models are likely to be seen for more complex reactions involving direct bridge bonds between adjacent dimers. In general, much larger cluster models which avoid such unphysical interactions would be needed to get reliable results for such complex systems. However, we can efficiently obtain results which should be comparable in

dx.doi.org/10.1021/ct3007259 | J. Chem. Theory Comput. 2012, 8, 5132−5136

accuracy to such more expensive calculations using our novel composite method.

5. CONCLUSIONS

We have defined a hybrid potential energy with which we can optimize the geometrical parameters on a sterically hindered cluster model representing the Si(100) surface. The hybrid energy effectively removes the unphysical intramolecular H···H interactions due to truncation of the reconstructed silicon surface. The located minima obtained for the initial interaction of allylic mercaptan on the Si(100) surface as well as some of the key transition states are described well with our new model. Overall, our composite energy method should be useful for many future applications involving chemistry on the Si(100) surface.

■ ASSOCIATED CONTENT

Supporting Information

The relaxed potential energy scan and the Cartesian coordinates for the subcalculations are provided. This material is available free of charge via the Internet at http://pubs.acs.org.

■ AUTHOR INFORMATION

Corresponding Author

*E-mail: kraghava@indiana.edu.

Notes

The authors declare no competing financial interest.

■ ACKNOWLEDGMENTS

The authors acknowledge support from NSF grant CHE-0911454 and Indiana University.

■ REFERENCES

(1) Higashi, G. S.; Chabal, Y. J.; Trucks, G. W.; Raghavachari, K. *Appl. Phys. Lett.* **1990**, *56*, 656−658.
(2) Buriak, J. M. *Chem. Rev.* **2002**, *102*, 1272−1308.
(3) Raghavachari, K.; Halls, M. D. *Mol. Phys.* **2004**, *102*, 381−393.
(4) Vreven, T.; Byun, K. S.; Komáromi, I.; Dapprich, S.; Montgomery, J. A.; Morokuma, K.; Frisch, M. J. *J. Chem. Theory Comput.* **2006**, *2*, 815−826.
(5) Vreven, T.; Morokuma, K.; Farkas, Ö.; Schlegel, H. B.; Frisch, M. J. *J. Comput. Chem.* **2003**, *24*, 760−769.
(6) Svensson, M.; Humbel, S.; Froese, R. D. J.; Matsubara, T.; Sieber, S.; Morokuma, K. *J. Phys. Chem.* **1996**, *100*, 19357−19363.
(7) Gamoke, B. C.; Mayhall, N. J.; Raghavachari, K. *J. Phys. Chem. C* **2012**, *116*, 12048−12054.
(8) Mayo, S. L.; Olafson, B. D.; Goddard, W. A. *J. Phys. Chem.* **1990**, *94*, 8897−8909.
(9) Frisch, M. J.; Trucks, G. W.; Schlegel, H. B.; Scuseria, G. E.; Robb, M. A.; Cheeseman, J. R.; Scalmani, G.; Barone, V.; Mennucci, B.; Petersson, G. A.; Nakatsuji, H.; Caricato, M.; Li, X.; Hratchian, H. P.; Izmaylov, A. F.; Bloino, J.; Zheng, G.; Sonnenberg, J. L.; Hada, M.; Ehara, M.; Toyota, K.; Fukuda, R.; Hasegawa, J.; Ishida, M.; Nakajima, T.; Honda, Y.; Kitao, O.; Nakai, H.; Vreven, T.; Montgomery, J. A., Jr.; Peralta, J. E.; Ogliaro, F.; Bearpark, M.; Heyd, J. J.; Brothers, E.; Kudin, K. N.; Staroverov, V. N.; Kobayashi, R.; Normand, J.; Raghavachari, K.; Rendell, A.; Burant, J. C.; Iyengar, S. S.; Tomasi, J.; Cossi, M.; Rega, N.; Millam, J. M.; Klene, M.; Knox, J. E.; Cross, J. B.; Bakken, V.; Adamo, C.; Jaramillo, J.; Gomperts, R.; Stratmann, R. E.; Yazyev, O.; Austin, A. J.; Cammi, R.; Pomelli, C.; Ochterski, J. W.; Martin, R. L.; Morokuma, K.; Zakrzewski, V. G.; Voth, G. A.; Salvador, P.; Dannenberg, J. J.; Dapprich, S.; Daniels, A. D.; Farkas, Ö.; Foresman, J. B.; Ortiz, J. V.; Cioslowski, J.; Fox, D. J. *Gaussian DV*, Revision H.08; Gaussian, Inc.: Wallingford, CT, 2010.
(10) Becke, A. D. *Phys. Rev. A* **1988**, *38*, 3098−3100.
(11) Becke, A. D. *J. Chem. Phys.* **1993**, *98*, 5648−5652.
(12) Lee, C.; Yang, W.; Parr, R. G. *Phys. Rev. B* **1988**, *37*, 785−789.
(13) Francl, M. M.; Pietro, W. J.; Hehre, W. J.; Binkley, J. S.; Gordon, M. S.; DeFrees, D. J.; Pople, J. A. *J. Chem. Phys.* **1982**, *77*, 3654−3665.
(14) Hariharan, P. C.; Pople, J. A. *Theor. Chem. Acc.* **1973**, *28*, 213−222.
(15) Krishnan, R.; Binkley, J. S.; Seeger, R.; Pople, J. A. *J. Chem. Phys.* **1980**, *72*, 650−654.
(16) Hossain, M. Z.; Kato, H. S.; Kawai, M. *J. Phys. Chem. B* **2005**, *109*, 23129−23133.
(17) Hossain, M. Z.; Kato, H. S.; Kawai, M. *J. Am. Chem. Soc.* **2008**, *130*, 11518−11523.
(18) Hossain, M. Z.; Kato, H. S.; Kawai, M. *J. Phys. Chem. C* **2009**, *113*, 10751−10754.
(19) Ferguson, G. A.; Than, C. T.-L.; Raghavachari, K. *J. Phys. Chem. C* **2009**, *113*, 18817−18822.
(20) Ferguson, G. A.; Than, C. T.-L.; Raghavachari, K. *J. Phys. Chem. Lett.* **2010**, *1*, 679−685.